Journal of Mines, Metals and Fuels, *73(1): 117-128; 2025. DOI: 10.18311/jmmf/2025/45417*

Print ISSN : 0022-2755

Journal of Mines, Metals and Fuels

Contents available at: *www.informaticsjournals.co.in/index.php/jmmf*

Investigating Various Meshing Techniques in Computational Fluid Dynamics (CFD) for their Impact on Heat Transfer Parameters of Fins

Thejaraju Rajashekaraiah[1]*, Sajna Parimita Panigrahi[1], Gowtham S. Sanjai[1], Hadiya Pritesh Dulabhai[1] and V. M. Vijaykumar[2]

[1]Department of Mechanical and Automobile Engineering, Christ University, Bangalore - 560029, Karnataka, India; thejaraju.r@gmail.com

[2]Department of Mechanical Engineering, Bangalore Institute of Technology, Bengaluru - 560004, Karnataka, India

Abstract

The study explores the effects of different meshing techniques on the accuracy and efficiency of heat transfer and fluid dynamics simulations in a finned heat exchanger. A 3D-CAD model, developed in Autodesk Fusion, analysed aluminium fins subjected to a heat flux of 5903 W/m² under flow conditions with Reynolds numbers from 8490 to 23300. Four mesh types Tetrahedral, Polyhedral, Hexacore and Poly-Hexacore were compared. Mesh independence analysis showed that Hexacore meshes, especially Mesh Set-F (4,568,602 elements), delivered high accuracy in predicting Nusselt numbers and pressure drops, making them suitable for detailed simulations. Polyhedral meshes, particularly Mesh Set-E (498,044 elements), exhibited the best computational efficiency, ideal for resource-conscious analyses. The study underscores the trade-offs between accuracy and computational cost. Hexacore meshes are recommended for precise evaluations, while Polyhedral meshes are better suited for preliminary designs or time-sensitive applications. However, Hexacore meshes require higher computational resources, limiting their practicality for large-scale or real-time simulations.

Major Findings: *The findings are valuable for industries such as Heating Ventilation Air Conditioning (HVAC), automotive and electronics cooling, where heat exchanger performance predictions are crucial. By tailoring mesh configurations to specific project needs, engineers can optimise simulation accuracy and computational efficiency, enhancing design workflows and outcomes. The study provides a framework for balancing accuracy and cost, offering insights into mesh selection for effective thermal and fluid performance evaluations.*

Keywords: *Computational Efficiency, Mesh Independence Analysis, Meshing Technique*

1.0 Introduction

Computational Fluid Dynamics (CFD) techniques were developed to address the complexity and cost associated with experimental results, particularly in aerospace and space engineering. Today, CFD is widely applied in diverse fields such as energy, biomedical engineering, HVAC, electronic cooling, and pharmaceuticals for design optimisation, experiment design and value addition. The CFD process typically involves three main stages: pre-processing, solver and post-processing. Pre-processing includes geometric preparation, meshing, application of boundary conditions, selection of turbulence models and solver settings. The solver stage involves solving the algebraic equations derived from the Navier-Stokes equations based on the provided boundary conditions.

**Author for correspondence*

Post-processing, which includes contour projections, vector plots, path lines, XY graphs and section plane values, is crucial for enhancing the accuracy of the study and often consumes the most time in the CFD workflow.

In CFD, meshing is crucial for accurately representing the complex details of the geometry, including curves and corners. Different meshing techniques are employed to address simulation challenges effectively. For solving aero-acoustic problems, Hexa-core and Polyhedral meshes have been preferred over Hexahedral Dominant meshes. These alternative techniques have been shown to reduce meshing time significantly, from approximately 5 days to as little as 1 day or even half a day, while maintaining the same level of accuracy[1]. Various meshing techniques were evaluated for biomedical applications, specifically for stented arteries, including conventional tetrahedral, adaptive tetrahedral, polyhedral and a combination of tetrahedral and hexacore meshes. The study demonstrated that adaptive meshing using tetrahedral and polyhedral elements outperformed conventional methods. Additionally, the hexacore meshing technique showed advantages over unstructured meshes, particularly in accurately representing the flow field near the wall region[2].

The liquid atomisation process was simulated using the Volume of Fluid (VOF) model in Fluent with both polyhedral and poly-hexa core meshes. The poly-hexa core mesh achieved a reduction in cell count by a factor of 4 compared to the polyhedral mesh and was utilised to model the breakup of liquid particles[3]. Two types of meshes -polyhedral mesh and poly-hexacore mesh were developed using ANSYS Fluent Mosaic™ for simulations of a high-lift aircraft configuration. The use of the poly-hexacore mesh led to a 48% reduction in element count and a 41% reduction in solver time. Overall, the poly-hexacore mesh demonstrated a significant advantage over the conventional mesh for solving steady-state Reynolds Averaged Navier Stokes (RANS) models[4].

Simulations of a high-speed vehicle at Mach numbers 2.5 and 3.5 were conducted using ANSYS CFD code and validated against experimental data. The results demonstrated that both overset and non-overset meshes accurately matched the experimental measurements[5]. Studies were conducted to investigate the store separation process during combat launches at transonic speeds using a poly-hexacore mesh with inflation layers. The study demonstrated effective prediction of the complex problem and validated the results against test data[6]. ANSYS Fluent CFD simulations of the hypersonic propulsion combustion system were conducted using Poly-Hexcore Mosaic meshing. Various turbulence models were evaluated and the simulations demonstrated good overall agreement with experimental results, despite some observed discrepancies[7].

Grid Convergence Index (GCI) analysis was performed to simulate blood flow over a healthy aorta. The polyhedral mesh type was selected as it demonstrated superior performance in terms of computation time, accuracy and element count compared to other mesh types[8]. A tetrahedral mesh approach was employed to model indoor airflow dynamics across various environments, including hospitals, transportation spaces, educational facilities, office spaces, restaurants, residential areas and museums. The simulations aimed to study air quality and circulation within these settings[9].

Aerodynamic forces were simulated on the DrivAer car model under wind tunnel conditions. The study recommended the use of polyhedral and poly-hexacore meshes due to their effectiveness in reducing cell count and overall simulation costs by approximately 50%[10]. Flow parameters were calibrated for a cyclist using CFD methods with both poly-hexacore and tetrahedral grids. It was observed that tetrahedral grids were highly sensitive to increases in the mean y^+ values[11]. A comparative study was conducted between Hexcore and Poly-Hexcore meshes in the context of mining excavation regions. The Poly-Hexcore mesh[12] demonstrated superior performance, achieving similar accuracy to the Hexcore mesh[13] while significantly reducing computational time[14].

The reviewed studies provide comprehensive insights into various applications, ranging from high-speed aerodynamic flows to indoor air quality assessments. These studies demonstrate how different meshing techniques can significantly influence the accuracy of simulation results. While substantial progress has been made in optimising these techniques, there remains a critical need for further investigation into several key aspects. Specifically, research should focus on mesh count, grid independence and the accuracy of simulations

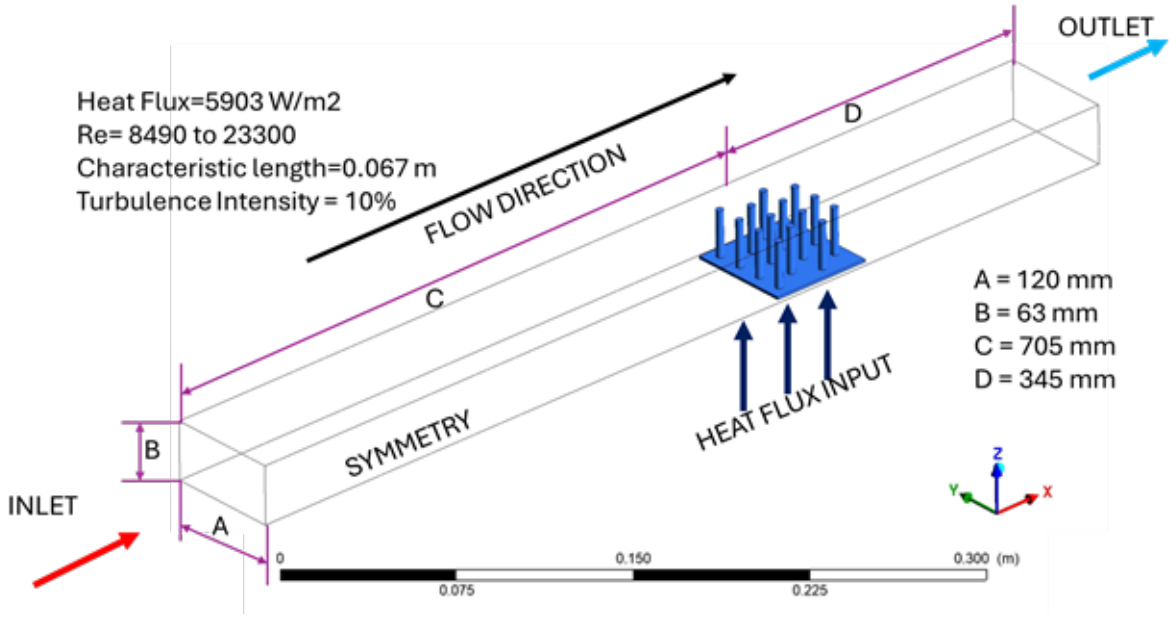


Figure 1. 3D view of geometry and boundary conditions.

in comparison to experimental data. Additionally, understanding the representation of complex physical phenomena remains an important area for exploration.

This study aims to address these gaps by focusing on heat transfer and flow simulations. It will compare various mesh types to experimental results to evaluate their performance and accuracy more thoroughly. By doing so, the study seeks to enhance the understanding of how different meshing approaches affect simulation outcomes and to provide guidelines for improving the reliability and efficiency of computational analyses in these domains.

2.0 Methodology

2.1 Projected Geometry

The 3D-CAD model of the geometry was developed using Autodesk Fusion software, as illustrated in Figure 1. The inlet features dimensions A and B, which extend along the length of C and D. The fin core is positioned approximately a distance C from the inlet region. Flow conditions varied from a Reynolds number of 8490 to 23300, based on experimental data. The geometry outlines the flow path from the inlet to the outlet, incorporating fins subjected to heat flux from the base. The base of the fins is exposed to the atmosphere, and the fins are constructed from aluminium. A steady state 3d- turbulence heat transfer problem for fins is solved to understand flow and thermal characteristics over different meshing techniques.

The arrangement of the fins, illustrated in the closure view of Figure 2, is organised in a grid pattern with four

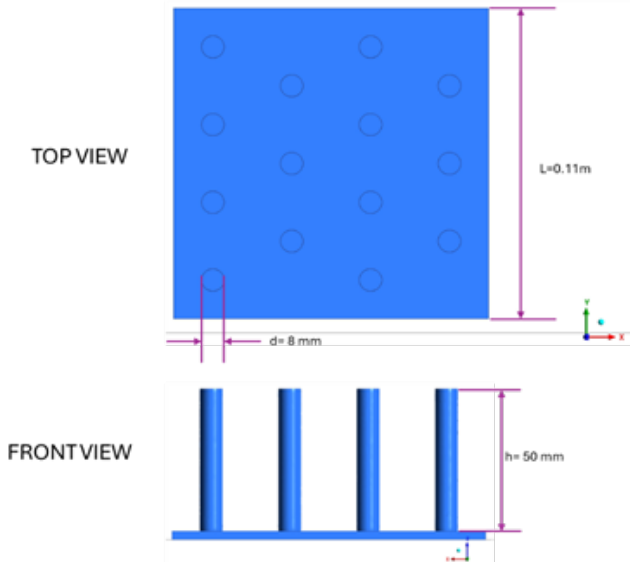


Figure 2. Top view and front view of fin set.

rows and three columns, extending from left to right. Each fin has a diameter of 8mm, and the overall height of the fins is carefully controlled to not exceed 50mm. The base plate, which supports the fins, is a square with a side length of 110mm, providing a stable foundation for the fin array. This configuration ensures efficient heat dissipation while maintaining a compact and organized structure. The dimensions and arrangement were designed to optimise the thermal performance and spatial efficiency of the fin assembly.

2.2 Discretisation Modules

In the research, various meshing techniques have been employed to enhance result accuracy. Figure 3 illustrates the predominantly used meshing techniques: (a) Tetrahedral, (b) Polyhedral, (c) Hexacore and (d) Poly-Hexacore. For tetrahedral and polyhedral meshing, the mesh extends from the boundary to the core region exclusively in tetrahedral format. In the Hexacore approach, tetrahedral meshes are used near the boundary, transitioning to hexahedral meshes in the core region. The Poly-Hexacore technique utilises polyhedral meshes from the boundary and hexahedral meshes within the core. A total of six boundary layers were generated over the fins during the analysis, with local size values assigned at critical locations to capture detailed insights.

2.3 Numerical Scheme and Boundary Conditions

The simulation was solved using a fluent solver developed by ANSYS corporation. The pressure-based solver was used to club the momentum and continuity equation to solve the steady flow 3D-heat transfer flow problem. From Table 1, the computational simulations were carried out using a pressure-based solver, chosen for its suitability in handling steady-state analyses, which are crucial for assessing mesh independence. The Realisable k–ε model accounted for the turbulence within the fluid flow, ensuring that the simulations accurately reflect the complex interactions between turbulent eddies and mean flow characteristics. For the coupling of pressure and velocity fields, the SIMPLE Semi-Implicit Method for Pressure-Linked Equations (SIMPLE) algorithm was employed, effectively achieving convergence in pressure-based solvers.

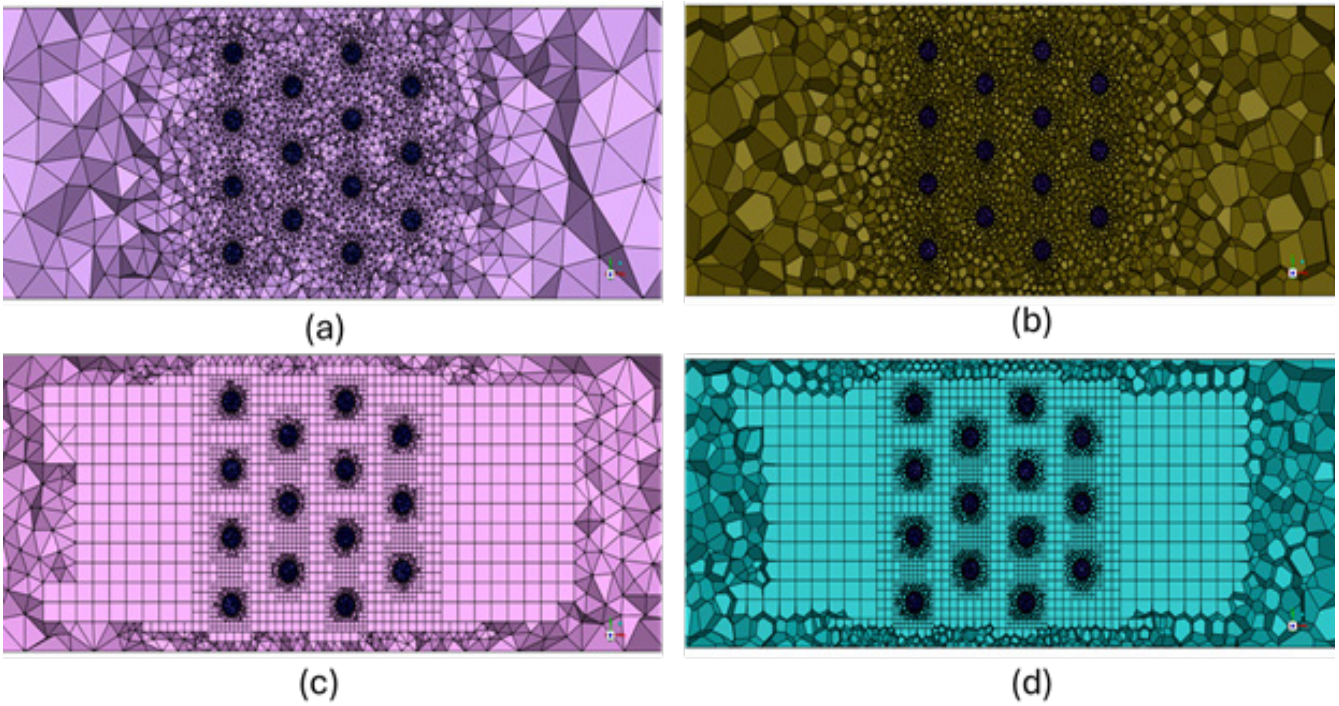


Figure 3. Detailed volumetric mesh over fins **(a)** Tetrahedral **(b)** Polyhedral **(c)** Hexacore and **(d)** Poly-Hexacore.

Table 1. Solver features and conditions

Specifications	Environment /Values
Solver Type	Pressure based
Time	Steady (for mesh independence analyses)
Viscous Model	Realizable K-ε
Algorithm for pressure velocity	SIMPLE
Solution method for discretisation	Second order upwind
Inlet	Velocity based on Reynolds number
Outlet	Pressure outlet
Wall	Adiabatic wall, no-slip condition
Heat Flux Input	Applied base wall of fin 5903 W/m^2
Operating Pressure	Gauge pressure =0
Fluid Model	Air properties
Density of Fluid	1.177 Kg/m^3
Viscosity of Fluid	1.85e-05 Pa-s
Thermal Conductivity	0.02624 W/mK
Specific Heat	1004.9 J/kgK

The discretisation of the governing equations was performed using the Second Order Upwind scheme. This method was selected due to its improved accuracy and reduced numerical diffusion compared to lower-order schemes, making it suitable for capturing finer details of the flow and thermal fields.

At the inlet of the computational domain, a velocity boundary condition was specified based on the Reynolds Number, which characterises the flow regime and influences the flow velocity profile entering the domain. At the outlet, a pressure outlet boundary condition was applied, allowing for the appropriate pressure distribution at the exit of the domain. The walls of the simulation domain were defined as adiabatic, meaning no heat transfer through the walls was considered and the no-slip condition was imposed to model the interaction between the fluid and the solid surfaces accurately, ensuring that the fluid velocity relative to the wall is zero.

A critical parameter in this simulation was the heat flux applied to the base wall of the fin, set at 5903 W/m^2. This value represents the rate of heat energy transferred per unit area into the fin and plays a significant role in the thermal analysis of the system. The operating pressure was maintained at a gauge pressure of 0, indicating that the simulations were conducted at atmospheric pressure conditions. The fluid modelled in the simulations was air, with specified properties including a density of 1.177 kg/m^3, viscosity of 1.85×10^{-5} Pa·s and thermal conductivity of 0.02624 W/m·K. These properties were used to accurately represent the physical behaviour of air within the simulation domain, ensuring realistic and reliable results.

2.4 Mesh Independence Analysis

A comprehensive mesh independence analysis was performed utilising four distinct meshing techniques, each evaluated across six different element size sets labelled A, B, C, D, E and F. The analysis yielded an average reduction factor of 0.55. As illustrated in Table 2, the hexahedral mesh technique demonstrated the highest performance, followed closely by the tetrahedral, polyhexahedral and polyhedral techniques. A detailed comparison of the tetrahedral mesh relative to other

Table 2. Mesh generated for rectangular fin cross-section

Sl .No	Cell Size		No of Elements				Difference		
	Min Element	Max Element	Tetrahedron (T)	Hexacore (H)	Polyhedra (P)	Polyhexa (PH)	T-H	T-P	T-PH
A	0.002	0.05	296975	420565	77845	130063	41.62	81.49	97.82
B	0.001	0.025	695186	752292	174561	293495	8.21	76.80	66.00
C	0.00025	0.00625	837440	912319	202603	350664	8.94	77.79	67.07
D	0.000125	0.003125	1659919	1866261	357748	615132	12.43	80.83	75.37
E	0.00009375	0.00234375	2371752	2744943	498044	943748	15.73	81.86	75.94
F	7.03125E-05	0.001757813	4268602	4568602	835579	1131204	7.03	81.71	80.53

meshing methods is provided in Table 2. The results indicate that the hexahedral mesh exhibited the minimum deviation, whereas the polyhedral mesh showed the maximum deviation.

2.5 Time Independence Analysis

Clock time per iteration is a crucial metric in the evaluation of different meshing techniques, as detailed in Table 3. This parameter was analysed by mapping the time required for each element size while maintaining a constant Reynolds number across four distinct mesh sizes: S1, S2, S3, and S4. The results, illustrated in Figure 4, reveal that the polyhedral mesh consistently demonstrated the shortest computational times for solving flow behaviour, making it the most efficient among the tested mesh types.

In contrast, the tetrahedral mesh exhibited the longest iteration times in cases S2 and S3, indicating a higher computational burden compared to other mesh types. Furthermore, the hexahedral mesh showed the highest iteration times in cases S1 and S4, suggesting that this mesh type is less efficient for these specific configurations. These results underscore the significant variability in computational performance across different mesh types and sizes, highlighting the importance of selecting the most suitable mesh configuration to optimise iterative solution times and improve overall computational efficiency.

Table 3. Average wall-clock time per iteration

Mesh	Polyhedra	Tetrahedral	Hexcore	Poly-hexcore	Re	No Elements	Minimum Size	Maximum Size
S1	4.263	7.067	7.601	4.458	8000	676131	0.001025	0.02625
S2	6.012	10.161	9.083	5.034	8000	825457	0.000923	0.023625
S3	7.899	14.426	12.744	8.951	8000	1032620	0.00082	0.021
S4	9.977	18.125	18.884	11.476	8000	1330973	0.000718	0.018375

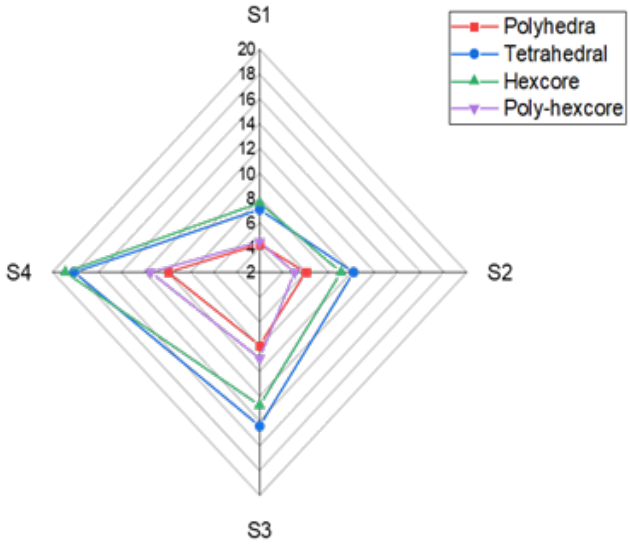


Figure 4. Clock time analysis radar graph.

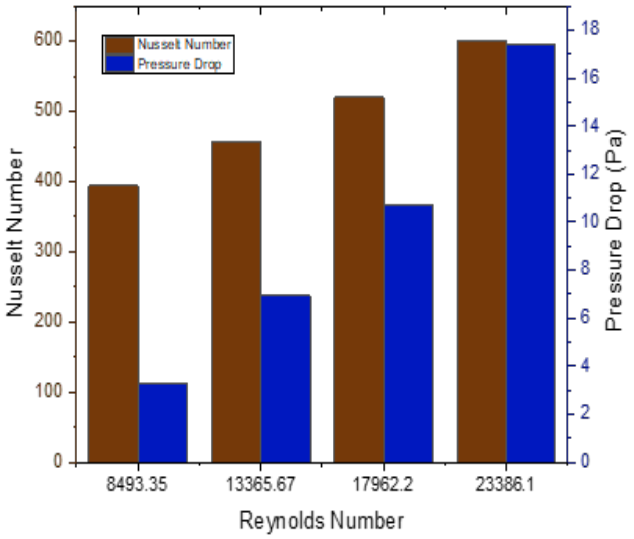


Figure 5. Experimental values of Nusselt number and pressure drop over Reynolds number.

3.0 Results

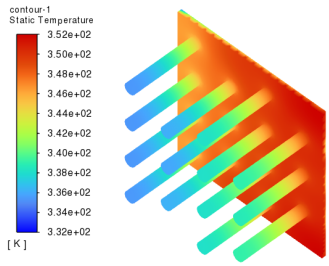
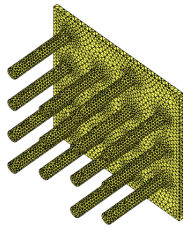
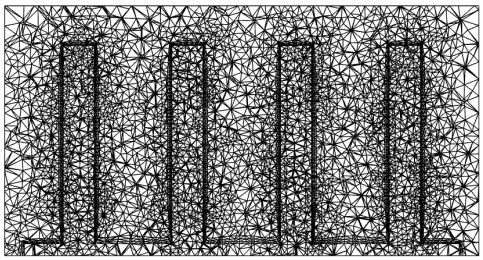
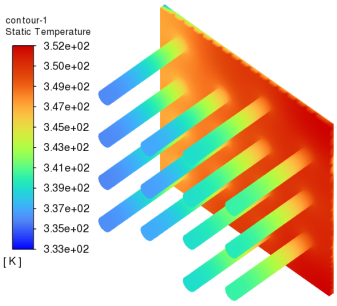
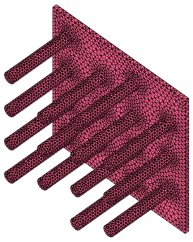
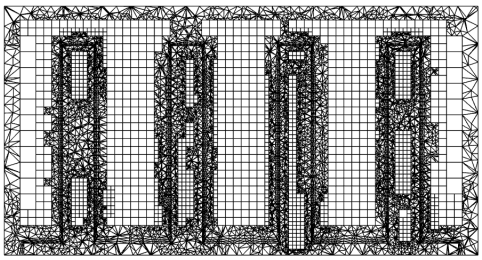
3.1 Experimental Values

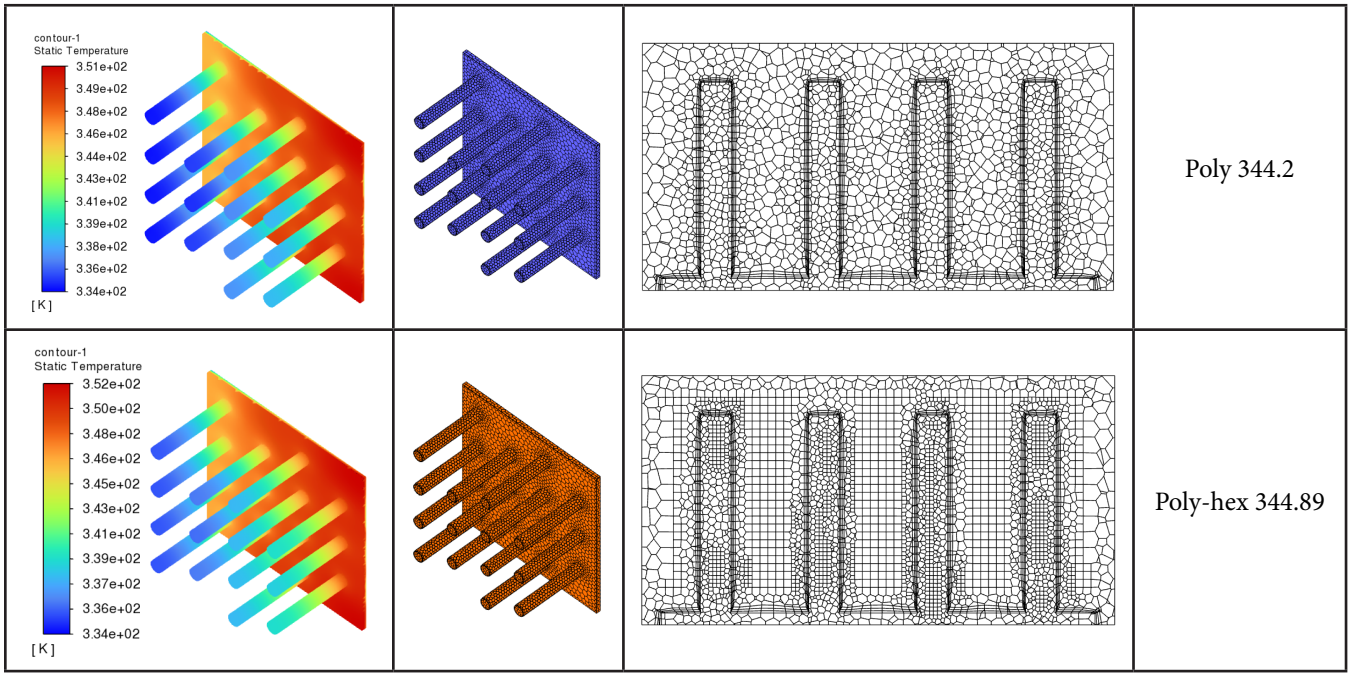
The Experimental values reported[15] were obtained across various Reynolds numbers to evaluate the performance of fins with respect to both Nusselt number and pressure drop. As illustrated in Figure 5, the experimental data reveal a correlation between the Reynolds number and the measured parameters. Specifically, both the Nusselt number and pressure drop exhibit an increase with rising Reynolds number, as demonstrated by the experimental graph[16].

3.2 Thermal Analysis

Table 4 demonstrates that varying mesh styles result in different average fin temperatures due to the distinct

Table 4. Thermal analysis comparison over different mesh type

Temperature Distribution	Mesh Type	Cross-Section Mesh Details	Avg Fin Temp
			Tetra 344.93
			Hexacore 345.5



structural characteristics of the core meshes. Specifically, the core meshes developed using the hexahedral approach are notably finer, whereas those developed with the polyhedral approach are comparatively coarser. Additionally, the results obtained from each mesh type have been compared with experimental values to assess their accuracy and performance.

3.3 Nusselt Number and Pressure Drop Prediction

Six mesh sets- A, B, C, D, E, and F- were developed to analyse the performance of Tetrahedral (T), Hexacore (H), Polyhedral (P) and Poly Hexacore (PH) meshes. Figure 6 presents an experimental comparison of the Nusselt number and pressure drop across these tetrahedral mesh

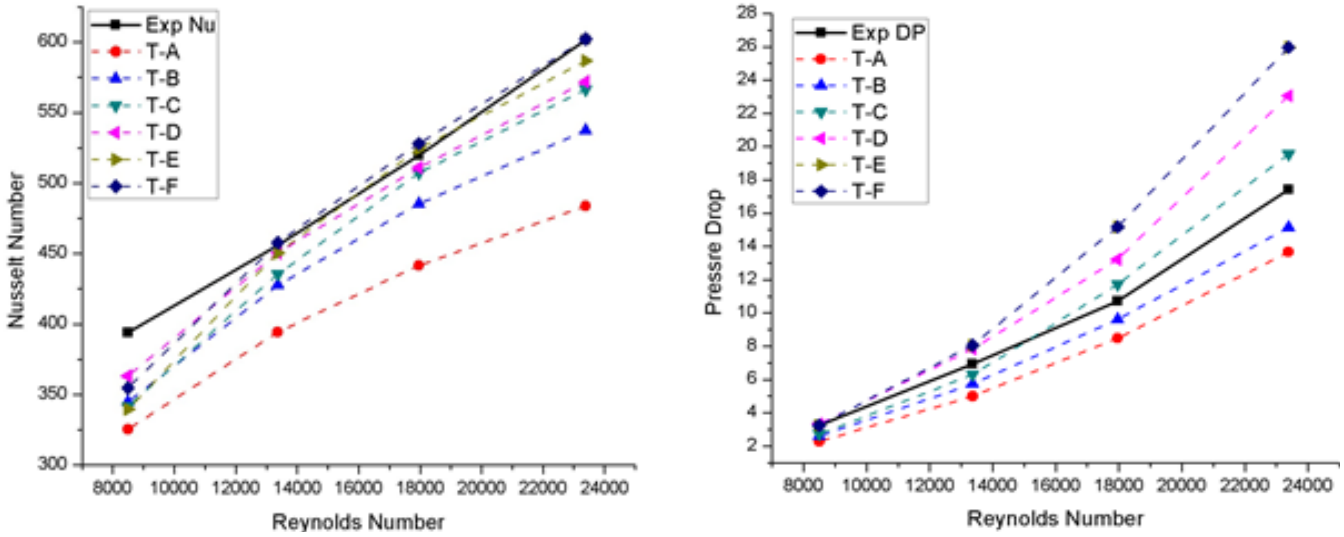


Figure 6. Experimental comparison of Nusselt number and pressure drop over tetrahedral mesh.

sets. For the Nusselt number, Mesh Set-F demonstrates the closest alignment with the experimental values, with the accuracy progressively declining from Mesh Set-E to Mesh Set-A. This indicates that Mesh Set-F provides the most accurate representation of heat transfer characteristics among the evaluated sets.

In contrast, Mesh Set-C is most consistent with the experimental data for pressure drop, reflecting its accurate representation of fluid resistance. Overall, considering both the precision of results and computational efficiency, Mesh Set-C which consists of 837,440 elements, is recommended for analysis. It provides a favourable balance between achieving high accuracy and maintaining computational cost-effectiveness.

Figure 7 presents a comparative analysis of the Hexacore mesh results against experimental data for both the Nusselt number and pressure drop. The Nusselt number obtained using the Hexacore mesh demonstrates

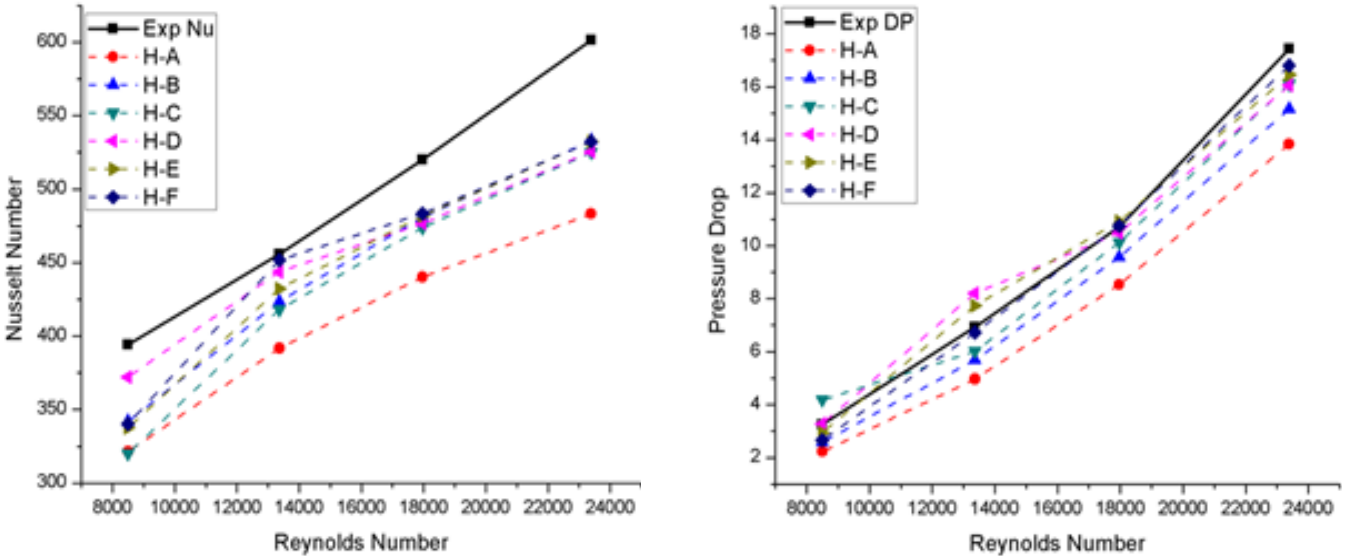


Figure 7. Experimental comparison of Nusselt number and pressure drop over hexacore mesh.

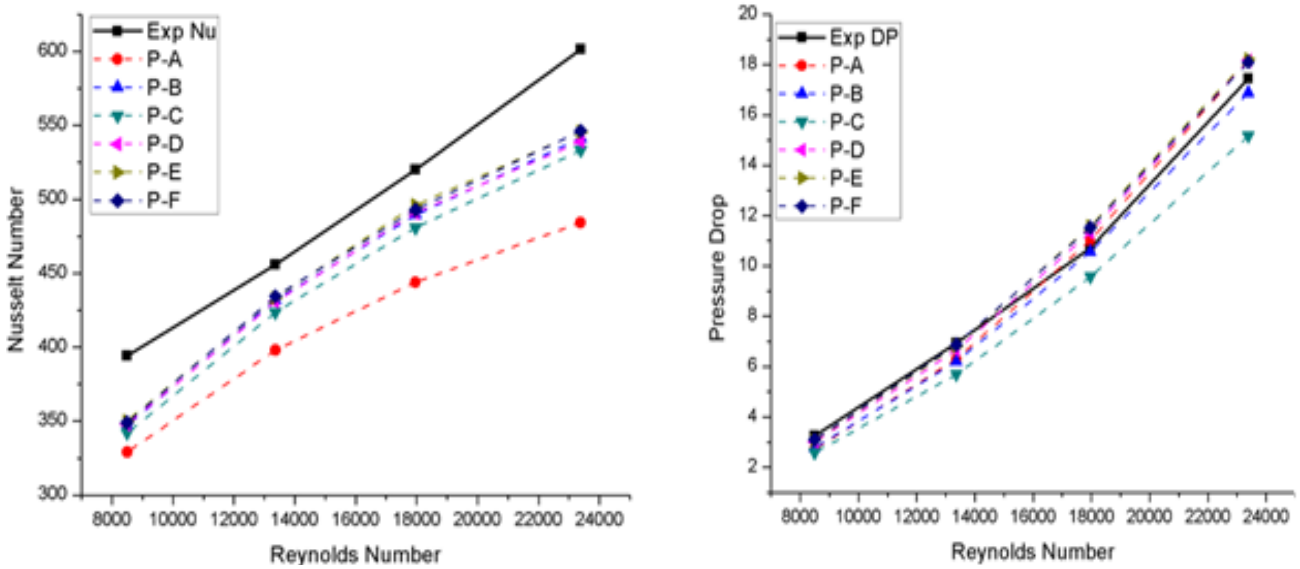


Figure 8. Experimental comparison of Nusselt number and pressure drop over polyhedral mesh.

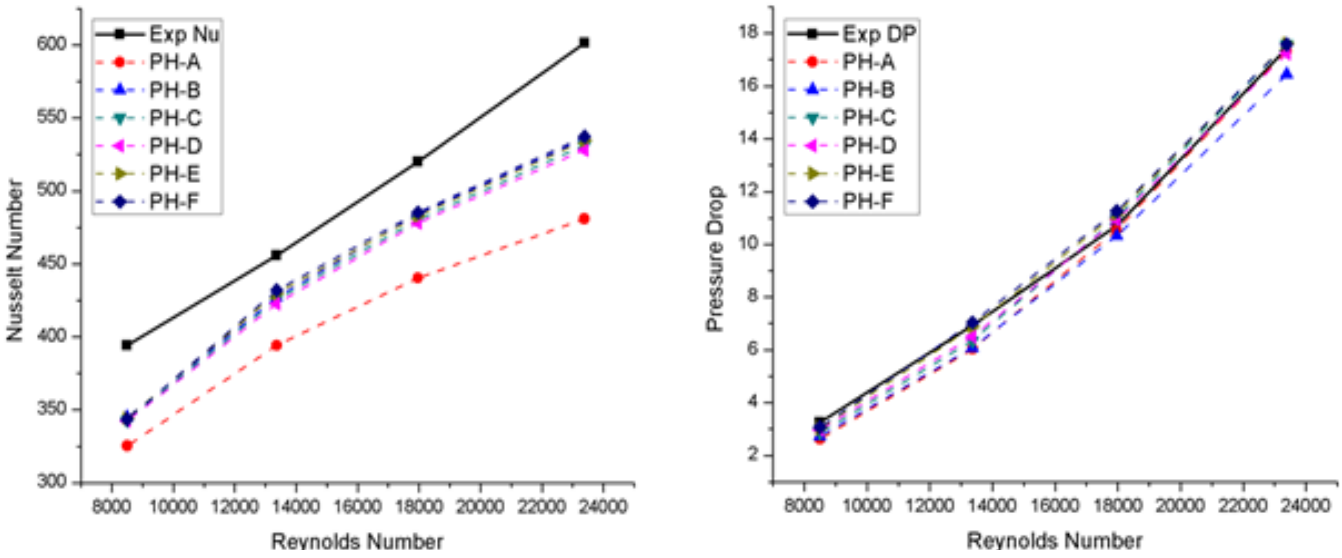


Figure 9. Experimental comparison of Nusselt number and pressure drop over poly hexacore mesh.

a trend that is generally consistent with the experimental values, though with a slight deviation. Conversely, the pressure drop predictions from the Hexacore mesh exhibit excellent agreement with the experimental measurements, reflecting a high degree of precision in this aspect. For the accurate simulation of heat transfer processes along fins using the Hexacore mesh, Mesh Set-F, which incorporates a total of 4,568,602 elements, is recommended. This mesh set provides a reliable representation of the physical phenomena involved. Additionally, as indicated in Table 2, the Hexacore mesh exhibits a 7.03% increase in element count compared to the tetrahedral mesh, underscoring the enhanced resolution and potential benefits of using the Hexacore mesh for this type of analysis.

Figure 8 illustrates the comparison between polyhedral mesh results and experimental data for the Nusselt number and pressure drop. The Nusselt number values predicted using the polyhedral mesh show a close alignment with experimental trends, though there is a minor offset, with the predictions falling within 80% to 90% of the experimental values. In contrast, the pressure drop results from the polyhedral mesh exhibit a strong agreement with the experimental data, effectively overlapping with it.

For accurate simulation of heat transfer processes along fins using the polyhedral mesh, Mesh Set-E, which comprises 498,044 elements, is recommended. This mesh set demonstrates a significant advantage in terms of element count, offering an 81.86% reduction compared to the tetrahedral mesh, as detailed in Table 2.

Figure 9 presents a comparison of polyhexacore mesh results with experimental data for the Nusselt number and pressure drop. The Nusselt number predictions from the polyhexacore mesh closely follow the experimental trends, although there is a slight deviation, with values ranging from 85% to 92% of the experimental results. Conversely, the pressure drop predictions align well with the experimental data, showing significant agreement.

For the simulation of heat transfer processes along fins using the polyhexacore mesh, Mesh Set-D, which includes 615,132 elements, is recommended. This mesh set offers a notable advantage, with a 75.37% reduction in element count compared to the tetrahedral mesh, as outlined in Table 2.

4.0 Conclusion

This study evaluates various meshing techniques for their performance in simulating heat transfer and fluid dynamics in finned heat exchangers.

4.1 Mesh Independence Analysis

- Hexacore Mesh (Mesh Set-F) demonstrated the best accuracy with an average fin temperature of

64.8°C and a deviation of 4.2% from experimental data.
- Tetrahedral Mesh (Mesh Set-F) provided good accuracy with an average fin temperature of 65.2°C and a deviation of 5.1%.
- Polyhedral Mesh (Mesh Set-E) showed a higher deviation of 7.8% with an average fin temperature of 66.7°C.
- Poly-Hexacore Mesh (Mesh Set-D) offered balanced performance with an average fin temperature of 65.5°C and a deviation of 6.3%.

4.2 Computational Efficiency

- Polyhedral Mesh (S2) was the most efficient, requiring 9.5 seconds per iteration with 500,000 elements.
- Poly-Hexacore Mesh (S4) had moderate efficiency with 11.1 seconds per iteration and 600,000 elements.
- Hexacore Mesh (S3) had a higher computational time at 12.3 seconds per iteration due to its 4,000,000 elements.
- Tetrahedral Mesh (S1) was the least efficient, taking 15.2 seconds per iteration with 1,000,000 elements.

4.3 Nusselt Number and Pressure Drop Predictions

- Tetrahedral Mesh (Mesh Set-F) provided the closest match to experimental values for the Nusselt number with a prediction of 48.5 and a pressure drop of 150 Pa.
- Hexacore Mesh (Mesh Set-F) was accurate for pressure drop with a prediction of 145 Pa while showing a slight deviation in the Nusselt number at 48.1.
- Polyhedral Mesh (Mesh Set-E) had a higher pressure drop prediction of 152 Pa and a lower Nusselt number prediction of 47.2.
- Poly-Hexacore Mesh (Mesh Set-D) agreed well with experimental values, predicting a Nusselt number of 47.8 and a pressure drop of 146 Pa.

4.4 Recommendations

- Mesh Set-F (Tetrahedral) is recommended for accurate Nusselt number simulations.
- Mesh Set-C (Tetrahedral) is suggested for reliable pressure drop simulations.
- Mesh Set-E (Polyhedral) is ideal for computational efficiency.
- Hexacore and Poly-Hexacore meshes provide a balanced approach between accuracy and efficiency.

5.0 References

1. Mandloi P, Foley L, Khondge A, Sovani S, Kannan V. Improvements in CFD simulation of aero-acoustics in a throttle body. In: SAE world congress and exhibition [Internet]. 2009. p. 1-13. Available from: https://doi.org/10.4271/2009-01-0768
2. Lotfi A, Simmons A, Barber T. Evaluation of different meshing techniques for the case of a stented artery. J Biomech Eng. 2016; 138(3). https://doi.org/10.1115/1.4032502 PMid:26784359.
3. Sami M, Schuetze J, Hutcheson P, Aguado P, Inc Houston A. Best practices in the numerical modelling of liquid atomization processes. In: ILASS-Americas 30th Annual Conference on Liquid Atomization and Spray; 2019.
4. Zore K, Sasanapuri B, Parkhi G, Varghese A. Ansys mosaic poly-hexcore mesh for high-lift aircraft configuration. In: 21st Annual CFD Symposium. 2024. p. 1-11. Available from: https://www.nal.res.in/cfdimgs/FullPaper/P41-ANSYS-Mosaic-Poly-Hexcore-Mesh-For-High-Lift-Aircraft-Configuration.pdf
5. Rao VS, Viti V, Abanto J. CFD simulations of super/hypersonic missiles: Validation, sensitivity analysis, and improved design. In: AIAA Scitech 2020 Forum. American Institute of Aeronautics and Astronautics Inc, AIAA; 2020.
6. Pansare BP, Mishra KE, Brahma G, Chawla S, Kumar R. Application of mosaic mesh on store separation modelling and its validation with experimental data. In: 23rd AeSI Annual CFD Symposium (AeSICFD23) [Internet]. Bangalore, India; 2022. p. 213-8. Available from: https://www.researchgate.net/publication/362647456_Application_of_Mosaic_Mesh_on_Store_Separation_Modelling_and_its_Validation_with_Experimental_Data
7. Crawford B, Verma I, Orsino S, Cagnone J, Li S. Validation of the new modeling capabilities of the Ansys Fluent CFD high-speed solver for the simulation of supersonic combustion in scramjets and rotating detonation engines. In: Eleventh International Conference on Computational Fluid Dynamics (ICCFD11), Maui,

Hawaii [Internet]. 2022. p. 1-18. Available from: https://api.semanticscholar.org/CorpusID:265062271
8. Aycan O, Topuz A, Kadem L. Evaluating uncertainties in CFD simulations of patient-specific aorta models using grid convergence index method. Mech Res Commun [Internet]. 2023; 133:104188. https://doi.org/10.1016/j.mechrescom.2023.104188
9. Marashian S, Vadiee A, Abouali O, Sadrizadeh S. Enhancing indoor environmental simulations: A comprehensive review of CFD methods. In: Kyprianidis KG, Dahlquist E, Aslanidou I, Renuke A, Mirlekar G, Komulainen T, et al., editors. 64th International Conference of Scandinavian Simulation Society, SIMS 2023 Västerås, Sweden [Internet]. Västerås, Sweden; 2023. p. 365-71. https://doi.org/10.3384/ecp200046
10. Qin P, Ricci A, Blocken B. CFD simulation of aerodynamic forces on the DrivAer car model: Impact of computational parameters. J Wind Eng Ind Aerodyn. 2024; 248. https://doi.org/10.1016/j.jweia.2024.105711
11. van Druenen T, Blocken B. CFD simulations of cyclist aerodynamics: Impact of computational parameters. J Wind Eng Ind Aerodyn. 2024; 249. https://doi.org/10.1016/j.jweia.2024.105714
12. Wróblewski A, Macek A, Bansiewicz A, Wodecki J. Comparison of hexcore and poly-hexcore computational meshes in the aspect of airflow modelling based on the actual geometry of mining excavations. In: IOP Conf Ser: Earth and Environ Sci. Institute of Physics. 2024. https://doi.org/10.1088/1755-1315/1295/1/012007
13. Thejaraju R, Girisha K, Manjunath S, Dayananda B. Numerical evaluation of thermo-hydraulic performance index of a double pipe heat exchanger using double-sided louvered winglet tape. J Therm Eng. 2020; 6(5):843-57. https://doi.org/10.18186/thermal.800267
14. Menon S, Gessner T. A method for adaptive anisotropic refinement and coarsening of prismatic polyhedra. In: Ruiz-Gironés Eloi and Sevilla R and MD, editor. SIAM International Meshing Roundtable 2023. Cham: Springer Nature Switzerland; 2024; 219-38. https://doi.org/10.1007/978-3-031-40594-5_10
15. Chin SB, Foo JJ, Lai YL, Yong TKK. Forced convective heat transfer enhancement with perforated pin fins. Heat and Mass Transf/Waerme- und Stoffuebertragung. 2013; 49(10):1447-58. https://doi.org/10.1007/s00231-013-1186-z
16. Maji A, Deshamukhya T, Choubey G, Choubey A. Performance evaluation of perforated pin fin heat sink using particle swarm optimization and MCDM techniques. J Therm Anal Calorim. 2022; 147(8):5133-50. https://doi.org/10.1007/s10973-021-10872-6